Synthesis of Zinc Oxide Nanoparticles *via* Biomass of *Hypnea pannosa* as a Green Mediator and their Biological Applications

Yosra A. Modafer *

The biological manufacturing of zinc oxide nanoparticles (ZnO-NPs) using renewable sources is safe, harmless, and compatible with the environment. The capacity of *Hypnea pannosa* to synthesize ZnO-NPs was investigated in this work. Ultraviolet visible (UV-Vis) spectroscopy, transmission electron microscopy (TEM), Fourier transform infrared (FTIR) spectroscopy, dynamic light scattering (DLS), X-ray diffraction (XRD), and zeta potential analysis were employed to characterize the ZnO-NPs. The created ZnO-NPs showed antimicrobial activity against *Staphylococcus aureus*, *Enterococcus faecalis*, *Klebsiella pneumoniae*, *Acinetobacter baumannii*, *Candida albicans*, and *Candida auris*. ZnO-NPs showed an MIC of 12.5 µg/mL against *S. aureus, E. faecalis, K. pneumoniae, C. albicans*, and *C. auris*, but it had a 25 µg/mL against *Acinetobacter baumannii*. ZnO-NPs' ability to scavenge free radicals was assessed using the 1,1-diphenyl-2-picryl hydrazyl (DPPH) technique with IC_{50} of 36.2 µg/mL. Anti-inflammatory activity of ZnO-NPs compared to indomethacin at 1000 µg/mL was investigated, where the membrane's maximum stabilizer was 93.3%. ZnO-NPs demonstrated anticancer activity against PC3 and Caco2 cell lines with IC_{50} of 174.3 µg/mL and 83.3 µg/mL, respectively. Furthermore, ZnO-NPs demonstrated a range of anti-biofilm activities against *Pseudomonas aeruginosa* and *Staphylococcus aureus*. Furthermore, ZnO-NPs showed encouraging antiviral effect versus COX B4 as well as HSV1 with antiviral activities of 54.8% and 61.1%, respectively.

DOI: 10.15376/biores.19.2.3771-3792

Keywords: ZnO-NPs; Antimicrobial; Antioxidant; Biosynthesis; Biomass, Algae

*Contact information: Department of Biology, College of Science, Jazan University, P.O. Box. 114, Jazan 45142, Kingdom of Saudi Arabia; * Corresponding author: Ymodafer@jazanu.edu.sa*

INTRODUCTION

The application of nanotechnology within the area of chemistry, pharmaceuticals, as well as biotechnology is rapidly growing (Alghonaim *et al*. 2024a; Abdelhady *et al*. 2024). Specific advancements in gene transportation, nanomedicine, biological sensing, drug delivery, and numerous other applications are possible with this technology (Al-Rajhi *et al*. 2022; Abdelghany *et al*. 2023a). Strong surface-to-volume ratios are among the distinctive features of nanotechnologies that render particles with nano sizes fascinating (Hemaid *et al*. 2021; Alghonaim *et al*. 2024b). Nanoparticles (NPs) tend to be responsive compared to bulk substances because of unique features of NPs such as high surface area to volume ratios, low melting points, and excellent mechanical strength optical and magnetic properties (Alsalamah *et al*. 2023).

Several methods are used to create NPs, including biological, chemical, and physical. However chemical and physical methods can have harmful effects on human health and the environment. An attractive method in the current decade is biological processing to generate NPs. This approach is generally affordable, safe, and sustainable (Abdel Ghany *et al*. 2018; Al-Rajhi and Abdelghany 2023; Qanash *et al*. 2023). Resources found in nature, such as plant organs including leaves, roots, or flowers, along with various types of microorganisms such as bacteria, fungi, and algae are all environmentally acceptable sources for the synthesis of nanoparticles (NPs) (Agarwal *et al*. 2017; Singh *et al*. 2023).

Green synthesis techniques have recently been used to produce a variety of NPs of zinc, copper, silver, nickal, and gold (Priyadharshini *et al*. 2014; Salama *et al*. 2021). Among these, zinc oxide nanoparticles (ZnO-NPs) play an important role in biological systems. ZnO-NPs have been associated with other several applications such as electrochemical systems, cosmetics, rubber, pharmaceuticals, chemical fiber, and electronics (Agarwal *et al*. 2017). Algae represent the main safe sources that can be used in the preparation of NPs. They contain several metabolites such as proteins, alkaloids compounds, phenolic, vitamins, tannins, coenzyme-based intermediary molecules, saponins, as well as flavonoids. These metabolites can serve as reducing and stabilizing agents for various NPs formulations (Nagarajan *et al*. 2013; Alsalamah *et al*. 2023). Specifically, among the various functional groups that are present in flavonoids, the -OH group are considered to be principally responsible on limiting the incorporation of metal ions during the formation of the nanoparticles (Elrefaey *et al*. 2022; Alsalamah *et al*. 2023). Algae such as *Sargassum myriocystum*, *Calerpa peltata*, and *Hypnea valencia* were used in order to produce ZnO-NPs. ZnO-NPs production was shown to be rapid and persistent when the brown alga *S. myriocystum* was used (Azizi *et al*. 2014). Numerous investigators have documented the medicinal value of seaweeds' secondary metabolites and their synthesized NPs, such as anti-inflammatory, anti-tumor, antibacterial, antiviral, and anti-diabetic effects (Anjali *et al*. 2021; Alsalamah *et al*. 2023). The one reason for persistence of antibiotic-resistant microorganism is the over-usage of antibiotics; there is a need for research resources and expertise to create antibiotic-resistant microorganisms (Khan *et al*. 2016; Waters *et al*. 2016). In addition to harboring immune system reactions, the bacterial cells that are surrounded by the framework of biofilm show increased resistance to the current antimicrobial treatment. Because of this intricate network, bacteria are more likely to become resistant to an extensive range of medications, rendering traditional antibiotics ineffective (Ashajyothi *et al*. 2016; Jayabalan *et al*. 2019). Thus, the demand for next generation antibacterial, anticancer, and antiviral agents is growing, especially since the COVID-19 pandemic first appeared (Abdel Ghany *et al*. 2021). Researchers have looked at the mechanism by which ZnO-NPs limited the growth of several microorganisms, including *Escherichia coli*, *Candida albicans*, *Staphylococcus aureus*, *Klebsiella pneumonia*, *Bacillus subtilis*, *Sarcina lutea*, *Pseudomonas vulgaris*, *Pseudomonas aeruginosa*, and *Bacillus megaterium*. They found that ZnO-NPs first penetrated the cell wall. Subsequently they caused cell membrane disruption, and finally accumulation throughout the cytoplasm, which eventually causes cell's death. In addition to its antibacterial properties, ZnONP-based biological capabilities have been observed that include anti-diabetic, anti-inflammatory, anti-aging, antioxidant and anti-cancer properties (Siddiqi *et al*. 2018; Nagaraja *et al*. 2019).

The algae, *Hypnea pannosa* was selected in the present study as a mediator of ZnO-NPs synthesis for several reasons. First, it is a renewable resource. Second, as an autotroph,

it may grow without a synthetic medium. Finally, *H. pannosa* can grow in contaminated water sources with metals and dyes. The aim of the current work was to synthesize ZnO-NPs *via* the alga *H. pannosa*. The next steps were to characterize the created ZnO-NPs and investigate their antimicrobial, antioxidant and anti-inflammatory, antitumor, antibiofilm, and antiviral activities.

EXPERIMENTAL

Chemicals

The main chemical used in this experiment was zinc acetate dehydrate ($Zn(CH_3COO)_2 \cdot 2H_2O$), which was acquired through Sigma-Aldrich Co. (St. Louis, USA). Additional chemical substances, cultural media, and reagents that were utilized in the present investigations were acquired from Contemporary Lab Co., India.

Preparation of Algal Filtrate

After removing the salt dearies *via* washing with distilled water several times (up to 5 times), the seaweed of *Hypnea pannosa* (belong to macroalgae) was air-dried and milled into an extremely fine powder. Employing a magnetic stirring device, the amount of 10 g of algal biomass and 100 mL of water that had been distilled were mixed and warmed to 60 ℃ for 30 min, and then left to shake overnight. After a filtering by Whatman no.1 filter paper, the resultant solution was cooled and kept throughout the biosynthesis procedure (Alsalamah *et al*. 2024).

Gas Chromatography-Mass Spectroscopy (GC-MS) Analysis

Utilizing Agilent Technologies model 7890 (Santa Clara, CA, USA), gas chromatography-mass spectrometry (GC-MS) was used to identify the constituents of the *H. pannosa* ethanol extract. A gas chromatography system was used, equipped with a 30 m SPB-50 column with an inner diameter of 0.25 mm and a film 0.25 m thick. A temperature of 250 °C was chosen for the interface, while 230 °C was selected for injection. The ions source's temperature was calibrated at 200 °C. A constant flow rate of 1 milliliter per min was maintained while using helium as the container for the gas. The temperature protocol that was employed consisted of heating an oven isothermally for a total of five min at about 70 °C, raising the interior temperature approximately five degrees Celsius each min to 310 °C, followed by warming until a min at about 310 °C. The spectrum of mass was captured within a range of 50 to 600 *m*/*z* including a pair of scans every second. To examine the measurement spectrum, as well as chromatogram, a mass laboratories software was employed. Absorption duration and mass spectrum analysis were employed using a mass experiment approach that automatically counts the number of metabolite peaks. Utilizing Microsoft Excel, the formula was entered. The potential chemicals were found using the National Center for Biotechnology Information (NCBI) database (Yakubu *et al*. 2017).

ZnO-NPs Bio-production

ZnO-NPs were obtained using the biomass extract of *H. pannosa*. The reaction mixture required for ZnO-NPs production was prepared by mixing of 90 mL of 2 mM $Zn(CH_3COO)_2 \cdot 2H_2O$ solution with 10 mL of the *H. pannosa* extract in an Erlenmeyer flask. Conversely, 90 mL of 2 mM of Zn $(CH_3COO)_2 \cdot 2H_2O$ was mixed with 10 mL of

distilled water which served as a control. Also, distilled water was mixed with algal biomass extract alone as another control. All the prepared reaction mixtures in the flasks were left for 4 h under shaking conditions to form a homogenous mixture. These combinations underwent a 1-h incubation period at 70 °C and 150 rpm of continuous shaking. As a result, bio-reduced salt settled in the flask's bottom and took the form of a white precipitate. Decanting the supernatant resulted in the transfer of the powdery precipitate to 1.5 mL centrifuge tubes. Both samples were centrifuged for 30 min at 3000 rpm in order to wash them with distilled water. To assure the elimination of contaminants, the washing procedure was done three times (Naseer *et al*. 2020). ZnO-NPs were obtained preserved in a powder form at room temperature for additional study as well as biological activity assessment.

ZnO-NPs Characterization

The characterization of the produced ZnO-NPs was performed *via* a UV-Vis (UV-2100, UNICO, USA) spectroscopy (a range from 200 to 1000 nm). Fourier transform infrared spectrometer (FTIR) was employed for identifying potential functional groups of the molecules within the extract of *H. pannosa*. By applying FTIR spectroscopy (VERTEX 70 Spectroscopy, Japan), the measurement was carried out throughout the 4000 to 400 cm^{-1} spectral range. The ZnO-NPs were explored employing an X-ray difracto-meter, model X'Pert Pro (Philips, Eindhoven, Netherlands), running at 40 kV and 30 mA and fitted to have a Ni-filter/Cu-K emission ratio sensor (=1.5405). The crystalline nature of ZnO-NPs was explored at temperatures between 10 and 80 °C. The highest peak locations were determined and cross-referenced against the Joint Commission on Particulate Diffraction Standards (JCPDS) database. ZnO-NPs were evaluated employing TEM, which was the tool used for the morphological characterization and sample size calculations (JEOL 1010, Tokyo, Japan). The ZnO-NPs solution had been set on a specimen stage subsequently dripped across a carbon-coated Cu-grid with the goal to determine the substance being tested. Finally, The DLS as well as zeta potential analysis (Malvern, UK) produced the DLS and zeta potential. To make a homogenous solution, the ZnO-NPs were placed back in 25 ppm freshwater then vortexed. After that, the ZnO-NPs were put into a 1.5 mL solution of colloidal silver within a square cuvette for examination. The 0.1 to 1000 nm wavelength range was observed. The Zetasizer software was used to analyze ZnO-NPs data (Jan *et al*. 2020).

ZnO-NPs' Antimicrobial Activity Assessment by *via* Agar Well Method

A variety of human pathogenic microorganisms were employed in this experiment, including *Staphylococcus aureus, Enterococcus faecalis, Klebsiella pneumoniae, Acinetobacter baumannii, Candida albicans,* and *Candida auris*. Regarding microorganisms, nutrient broth was used for cultivation of bacterial cultures. The tested microbes were evenly distributed using Muller-Hinton agar on sterile petri dishes. Using a cork-borer that was sterilized, a 6-mm diameter well was created in the plates. To evaluate the antimicrobial assay, 100 µL of ZnO-NPs were added to the well. The plates were incubated for 24 h and 72 h at 37 and 30 °C, respectively, and then the zones of inhibition were evaluated. Every test was conducted 3 times, as in this reference with some modifications (Alsalamah *et al*. 2023).

Evaluation of the MBC and MIC Values

ZnO-NPs' minimum inhibitory concentrations (MIC) were determined using the technique of microdilution of broth *vs. Staphylococcus aureus*, *Enterococcus faecalis*, *Klebsiella pneumoniae*, *Acinetobacter baumannii*, *Candida albicans*, and *Candida auris*. Zinc oxide nanoparticles (NPs) were generated at different quantities (500, 250, 125, 62.5, 31.25, and 15.75 µg/mL) prepared by double fold serial dilution within Mueller Hinton (MH) broth. An inoculum size equivalent to 0.5 McFarland standard (20 µL) of microbial cell suspensions was added to all except the negative control well. Microbial solution was introduced to positive control wells to determine whether MH broth could sustain microbial growth. Sterility was ensured by using sterilized water from distillation and MH broth in the opposite control wells. Around 37 °C, these plates were allowed to incubate throughout a full day. Afterwards, 30 µL of resazurin solution (0.02% wt/v) (HiMedia) was then added into every well located on the plate and maintained again for a total of 6 h for the purpose of identifying the growth of bacteria. The hue changed from blue to red, indicating the presence of microbes. The microorganisms had grown adequately, as shown by the change in coloration to red in the growth control wells, and there was no indication of any contamination in the sterility control well based on any color fluctuation. By the modified microbroth dilution method, as reported by Ansari *et al*. (2015), the minimum bactericidal concentration (MBC) of ZnO-NPs against the tested pathogens was evaluated. The method employed for determining the MBCs used a twice-dilution technique with different concentrations (1000 to 7.81 µg/mL). The MBC was then determined by streaking the overnight-grown cultures from every single concentration onto plates filled with agar. A three-time run of the test yielded stated mean results.

Antioxidant Activity of ZnO-NPs

By implementing the 2,2-diphenyl-1-picrylhydrazyl (DPPH) method, the ability of nanoparticles to scavenge radicals was determined according to Alawlaqi *et al.* (2023) with some modification. A 0.1 mM DPPH suspension was created with 95% ethanol as the solvent, which was added to various ZnO-NPs concentrations (from 7.81 to1000 µg mL^{-1}) to begin a reaction. After shaking, the resulting mixtures were set aside in a dark place for 30 min at 25 °C. Following incubation, the resulting ascorbic acid had been used as a reference material, and at 517 nm absorption was read using a set of control samples (DPPH solution without sample) and 5 min of centrifugation. The following formula was utilized to ascertain ZnO-NPs' antioxidant capabilities: the scavenging capacity of DPPH (%) = (Absorbance of control – Absorbance of the sample)/ (Absorbance of control) ×100**.**

Anti-inflammatory Activities

Preparation of erythrocyte suspension and hypotonicity induced hemolysis

After it was taken from corresponding author of the current investigation in 3 mL heparinized tubes, the blood was centrifuged for 10 min at 3,000 rpm. A similar amount of regular saline that was partially included in the supernatant was used for disintegrating those red blood cell pellets. After measuring the total amount of the disintegrated red blood pellets, 40% v/v suspensions were made using an isotonic buffer mixture (10 mM sodium phosphate buffer, pH 7.4). The neutralizing liquid contained 0.2 g of NaH_2PO_4, 1.15 g of Na_2HPO_4, and nine grams of NaCl in one liter of distilled water. This was done using the blood cells of the patient that were recently regenerated (resuspended supernatant).

The hemolysis inhibition by ZnO-NPs was performed according to methods of Anosike *et al*. (2012) and Yahya *et al*. (2022) with some modification as follows: The ZnO-NPs sample utilized in the current study had been dispersed in distilled water, creating a solution that was hypotonic. ZnO-NPs (1000, 800, 600, 400, 200, and 100 µg/mL) were gradually added to an initial hypotonic solution (5 mL) in duplicated pairings (per dosage) of centrifuge chambers. Evaluated dosages of ZnO-NPs (100 to 1000 µg/mL) aqueous isotonic solution (5 mL) were additionally included to generate two pairs (per dose) of tubes for the centrifuge. Five milliliters of distilled water, as well as indomethacin containing 200 µg/mL were found inside the control tubes. Every tube was filled with 0.1 mL containing erythrocyte suspended state, and it had been well mixed. The solutions had been centrifuged at 1,300 g for 3 min after being incubated for 1 h at room temperature (37 °C). A Spectronic (Milton Roy) spectrophotometer was implemented to measure the absorption (OD) of the Erythrocyte level in the supernatant around 540 nm. By taking the rate of hemolysis generated within the presence of water that has been distilled to 100%, the proportion of hemolysis had been computed. The percent inhibition of hemolysis by ZnO-NPs was calculated thus:

$$\% \text{ Inhibition of hemolysis} = 1-(OD2-OD1)/(OD3-OD1) *100 \quad (1)$$

where the OD1 means the absorbance of the treated sample in the isotonic solution, OD2 means the absorbance of treated sample in the hypotonic solution, while OD3 means the absorbance of the control treated sample in the hypotonic solution. Hemolysis % was assessment by regarding to heamolysis in distilled water (100%).

Cytotoxic and Anticancer Activity of ZnO-NPs *via* MTT Assay

Cytotoxicity of ZnO-NPs was determined *in vitro* on normal Vero cells (Organism: Cercopithecus aethiops, Tissue: Kidney, Cell type: Epithelial, Culture properties: Adherent, Disease: Normal, ATCC: CCL-81). While anticancer was performed on colon (Caco2) and prostate (Pc3 cells) (Organism: Homo sapiens Human, Disease: Adenocacinoma). 3-(4,5-dimethylthiazol-2-yl)-2,5-diphenyltetrazolium bromide (MTT) assay was performed to detect the cytotoxicity and anticancer activity of ZnO-NPs according to Alghonaim *et al*. (2023) with some modification: The utilized cell lines at 1×10^5 cells/mL (100 µL) were inoculated in 96-well containing MTP for 24 h till a complete monolayer sheet was developed. The developmental monolayer sheet had been removed once a consolidated sheet filled with tested cells. Then the resulting cell monolayer was washed with washing medium. Serial dilutions of the tested ZnO-NPs were prepared in a medium made from RPMI comprising % serum (preservation medium). Three wells were designated as reference wells, receiving just preservation medium, while different wells were examined with 0.1 mL for every dilution of ZnO-NPs. Then, the quantity of cells was determined at wavelength of 620 nm.

Anti-Biofilm Activity of Zno-NPs

ZnO-NPs' capacity was evaluated using the MTP method, taking into account small adjustments were made to prevent or lessen the biofilm accumulation associated with the clinical organisms *S. aureus* as well as *Pseudomonas aeruginosa*, which was shown to be a strong biofilm-producing organism (Alsolami *et al*. 2023). In short, the ZnO-NPs ramping doses were added within a MTP with flat bottom that contained tryptic soy broth medium (TSB) having 1% glucose. Test pathogens had been diluted 1:100 to provide an inoculum (1.5×10^8 CFU/mL). It was then placed onto MTP and incubated. The incubation

period lasted 48 h (about 2 days) at 37 °C. After that, the development frequency was established by spectrophotometry at 620 nm, and each MTP hole's planktonic cells were eliminated without endangering the biofilm that had already developed. Moreover, the wells were cleaned multiple times with PBS around pH 7.4 to remove any remaining cells of floating unrestricted cells. Methanol 95% was added to each well to create an equal amount of 200 µL to help in the establishment of the biofilm. Subsequently, crystal violet (CV) 0.3% was added about 200 µL of onto the identical wells, followed by incubation for 15 min between 20 and 25 °C. Furthermore, sterile water that had been distilled has been employed to delicately eliminate the remaining CV stain. To identify quantitative production of biofilm, adding about 200 µL of 30% acetic acid the solution to all wells. Finally, the Elx800 MP reader was utilized to read and calculate quantitatively.

Evaluation of Antiviral Activity of Zno-NPs

Using a 96-well plate, 10,000 cells were placed *via* 200 µL of medium in each well. Three of the holes were left unfilled for blank controls. For cells to be able to stick to the plate wells, incubation (37 °C, 5% CO_2) was carried out overnight. After one hour of incubation, an equal amount (1:1 v/v) of the viral solution and tested sample were examined. The viral/sample (100 µL) was suspended for 5 min at 150 rpm over an unstable table, followed by incubation for one day at 37 °C with 5% CO_2 to enable the virus to begin working. Twenty µL of MTT solution were added to the wells (96-well plate) containing medium, followed by shaking at 150 rpm for 5 min to fully incorporate the MTT throughout the medium. The plate was incubated at 37 °C with 5% CO_2 for 5 h. The medium in the plate wells was emptied *via* filter paper to remove any leftovers. The formazan (MTT biochemical products) was redissolved in 200 µL of DMSO. The developed cytopathic effect was measured at density 560 nm (Qanash *et al.* 2022).

RESULTS AND DISCUSSION

GC-MS Analysis

The obtained results of GC-MS analysis are shown in Table 1 and Fig. 1. Most of the hypothetical compounds in Table 1 exhibited over 90% compatibility to those in the NCBI database. Hexadecanoic acid (25.7%) and isopropyl myristate (18.3%) had the greatest content proportions in the *H. pannosa* ethanol extract, followed by á-sitosterol, methyl ester, phenylmethyl ester, octadecanoic acid, ergosta-5,22-dien-3-ol, (3á,22e,24s), stigmast-5-en-3-ol, (3á,24s), and cholest-5-en-3-ol (3á), with area% of 5.80, 5.47, 4.09, 3.67, 3.32, 1.84, 1.27, and 1.23%, respectively. These compounds and other metabolites may play a vital role in the creation of ZnONPs as mentioned in other investigations (Alsalamah *et al*. 2023; Alghonaim *et al*. 2024).

Table 1. GC-MS Analysis for the Identified Compounds in *H. pannosa* Extract

Molecular formula	Molecular weight (g/mol)	Peak area (%)	Compound name	RT*
$C_{16}H_{32}O_2$	256.42	25.74	N-hexadecanoic acid	53. 17
$C_{17}H_{34}O_2$	270.5	18.31	Isopropyl myristate	48. 37
$C_{29}H_{50}O$	414.71	5.80	á-Sitosterol	88. 40
$C_{17}H_{34}O_2$	270.45	5.47	Methyl ester	51. 53
$C_{19}H_{38}O_2$	298.5	4.09	Methyl stearate	57. 89
$C_{18}H_{36}O_2$	284.5	3.67	Octadecanoic acid	59. 44
$C_{14}H_{12}O_3$	228.24	3.32	Phenylmethyl ester	44. 94
$C_{28}H_{46}$	398.7	1.84	Ergosta-5,22-dien-3-ol, (3á,22e,24s)-	84. 91
$C_{29}H_{5}0O$	414.71	1.27	Stigmast-5-en-3-ol, (3á,24s)-	83. 07
$C_{37}H_{64}O_2$	540.9	1.23	Cholest-5-en-3-ol (3á)-	83. 95

*RT, Retention time

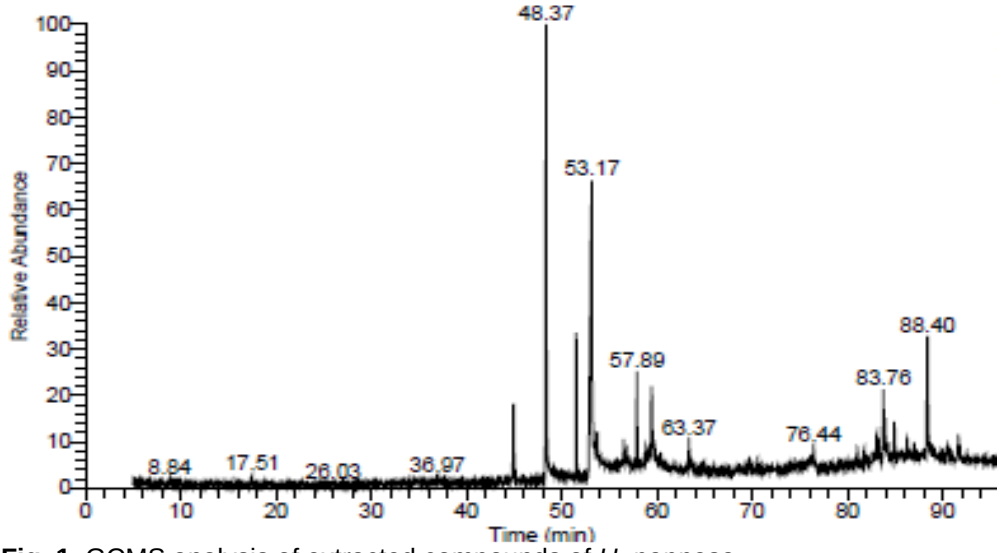

Fig. 1. GCMS analysis of extracted compounds of *H. pannosa*

Biosynthesis and Characterization of ZnO-NPs

ZnO-NPs had been synthesized using *H. pannosa* aqueous extract depending on its constituents. This procedure's main goal was to provide a clean, eco-friendly way to produce nanomaterials from *H. pannosa* extract (Fig. 2). Zinc salt was employed as a starting point for the generation of ZnO-NPs and was added to the *H. pannosa* extract until an incremental shift in the resultant color was noticed. The color shifted from brown to milky-white, indicating the creation of ZnO-NPs by the *H. pannosa* compared to the color of mixed distilled water with algal biomass extract or zinc acetate solution without algal biomass extract. The result of color change was agreement with another study (Talam *et al*. 2012).

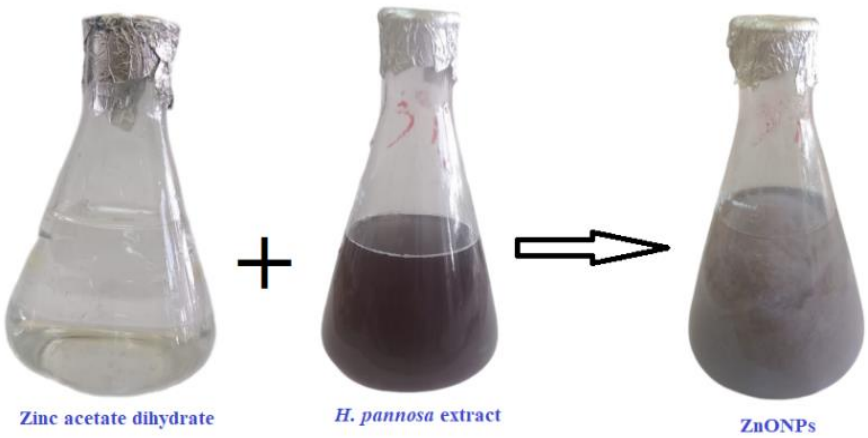

Fig. 2. Biosynthesize of ZnO-NPs from *H. pannosa* extract

A crucial method for verifying the formation and stability of metal NPs in aqueous solutions is UV-visible spectroscopy (Alsalamah *et al*. 2023, 2024).

In the present study, UV-Vis spectrum peak of synthesized ZnO-NPs was at 380 nm (Fig. 3), this maximum peak indicated the synthesis of ZnO-NPs. According to Jan *et al*. (2020), ZnO-NPs had significant UV spectrum absorption at 265 and 370 nm, which demonstrated the generation of ZnO-NPs.

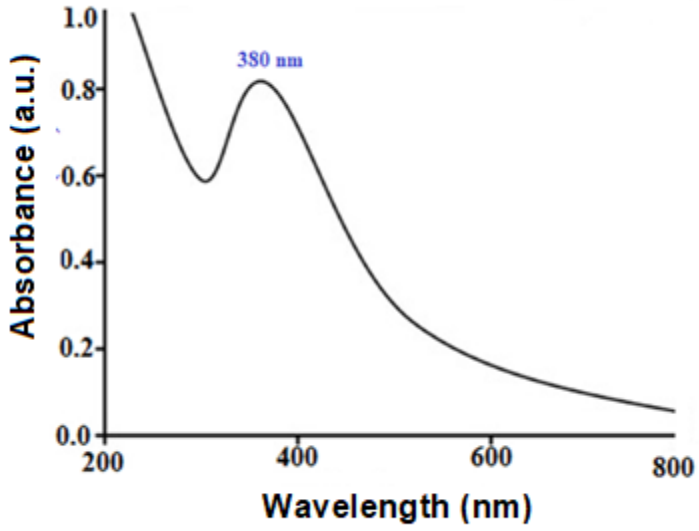

Fig. 3. UV–Vis absorption spectra of biosynthesized ZnO-NPs

With FTIR analysis, the functional groups mediated in ZnO-NPs synthesis can be described (Fig. 4). The signal at 3320, 1635, 1115, 1030, 960, 741, 596, and 513 cm^{-1} indicate the association of a capping agent *via H. pannosa* extract with ZnO-NPs. At 3385.4, 3291.8, and 3149.1 cm^{-1}, naturally occurring ZnO-NPs' FT-IR revealed distinct peaks (O–H, N–H stretching, aliphatic in amines that are primary, as well as O–H wide stretching) (Rahimi *et al*. 2020). It is significant to note that the Zn-O generation region corresponds to the FT-IR bands at 615.1 and 471.5 cm^{-1} (Kalaba 2021).

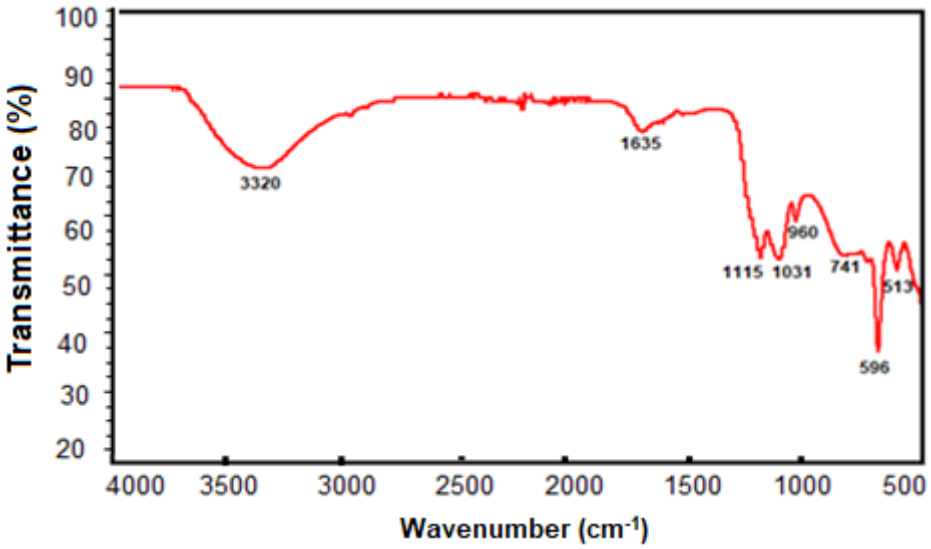

Fig. 4. FTIR spectral assay of analysis of biosynthesized ZnO-NPs

The X-ray diffraction pattern provided evidence to verify the crystalline character of the naturally produced ZnO-NPs. The characterization of ZnO-NPs by XRD shows five peaks at two θ values of 31.9°, 34.5°, 36.4°, 47.6°, and 56.7°, as shown in (Fig. 5).

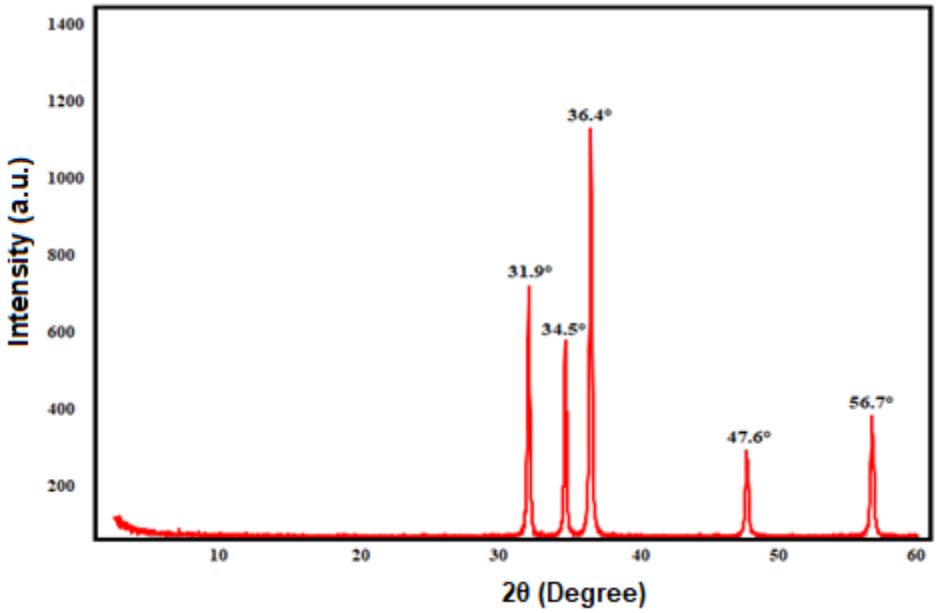

Fig. 5. X-ray diffraction (XRD) assay of biosynthesized ZnO-NPs

Using Scherrer's equation, the average diameters of the crystallite ZnO-NPs were determined. The ZnO-NPs sizes in this case ranged from 14.2 to 107.5 nm, which are in partial agreement with another study, where maximum ZnO-NPs size was 91.4 nm (Abdelhady *et al*. 2024).

The form, size, and particle size distribution of the biosynthesized ZnO-NPs were investigated using TEM and DLS. It was found that the size of ZnO-NPs ranged from 23 to 83 nm (Fig. 6). The obtained size in the current investigation may be depending on the

metabolites of *H. pannosa*. In another study, hexagonal form with an average of 42 nm was associated with ZnO-NPs created by aqueous extract of another alga namely *Sargassum muticum* (Azizi *et al*. 2014).

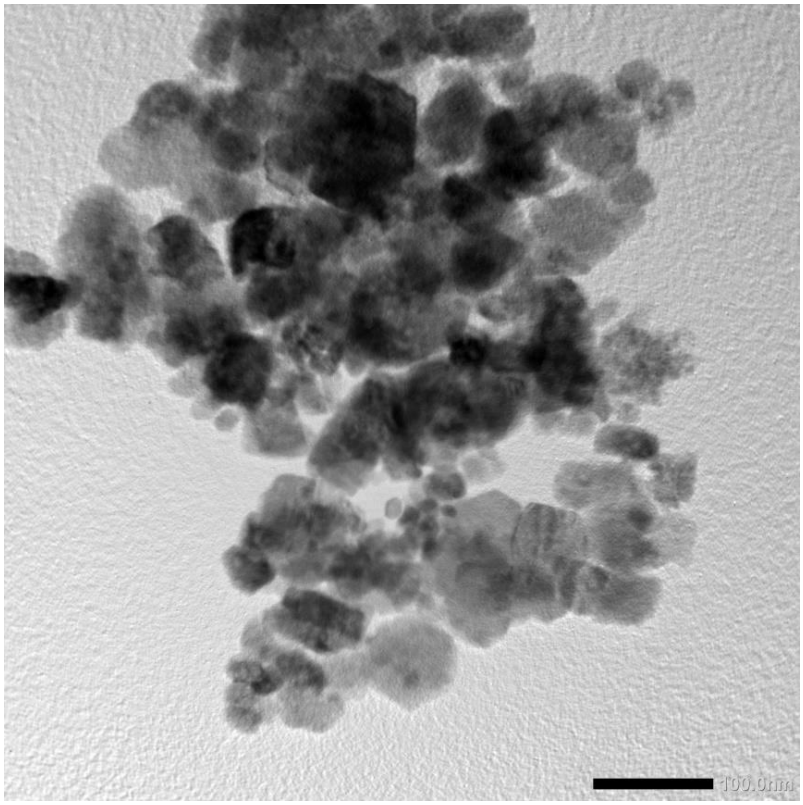

Fig. 6. TEM picture of biosynthesized ZnO-NPs (the NPs diameter was recorded on the basis of the size bar, 100 nm)

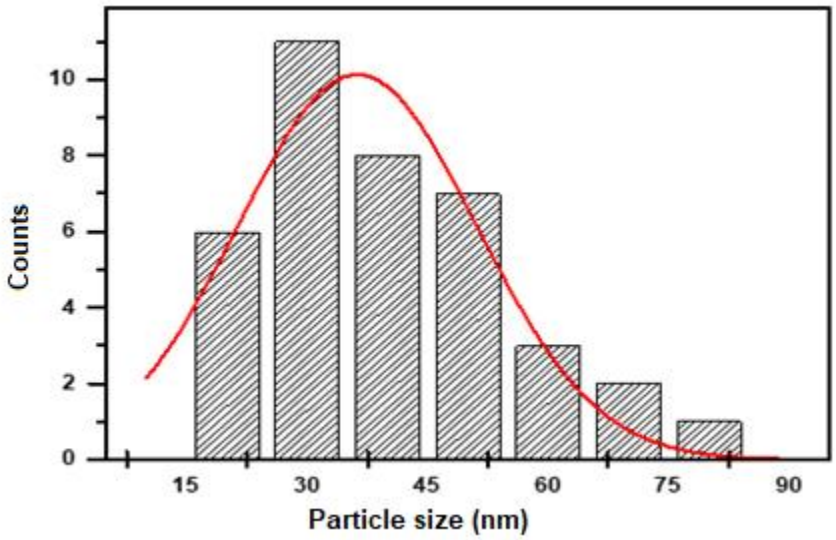

Fig. 7. DLS graph of biosynthesized ZnO-NPs

The mean size of the particle variations within the nano-sol obtained from DLS for ZnO-NPs created by *H. pannosa* extract are shown in Fig. 7. According to the obtained results, the average size of ZnO-NPs produced by *H. pannosa* with high polydispersity was 36.2 nm according to DLS analysis. The metabolites that absorbed on the surfaces of ZnO-NPs as stabilizer agents also had an impact on the sizes as determined via DLS, in addition to the metallic center of the NPs. The presence of enzymes, protein molecules, and carbohydrate could have been responsible for the variation in ZnO-NPs size, as these substances participate in the production and capping of nanoparticles in different ways (Kalaba *et al*. 2021).

Zeta potential is most often determined by the velocity at which particles move under the action of an applied electric field. Stability of of ZnO suspension is influenced by many factors according to Marsalek (2014), for example dispersant and pH. The mean zeta potential of ZnO-NPs was found to be -23 mV (Fig. 8). This suggests a colloidally stable suspension of ZnO-NPs. These observations provide evidence that components of the *H. pannosa* extract were functioning as stabilizers. The results showed strong agreement with another study (Kaur *et al*. 2022). The obtained findings suggest that the utilized precursor type of zinc salt can significantly affect the zeta potential of the created ZnO-NPs, which may be attributed to the surface charge and solubility of the zinc salts. Also, pH has been found to affect the zeta potential. For instance, Romdhane *et al.* (2015) mentioned that the zeta potential decreased for pH values less than 4, but it remained constant in the pH range from 4 to 8.

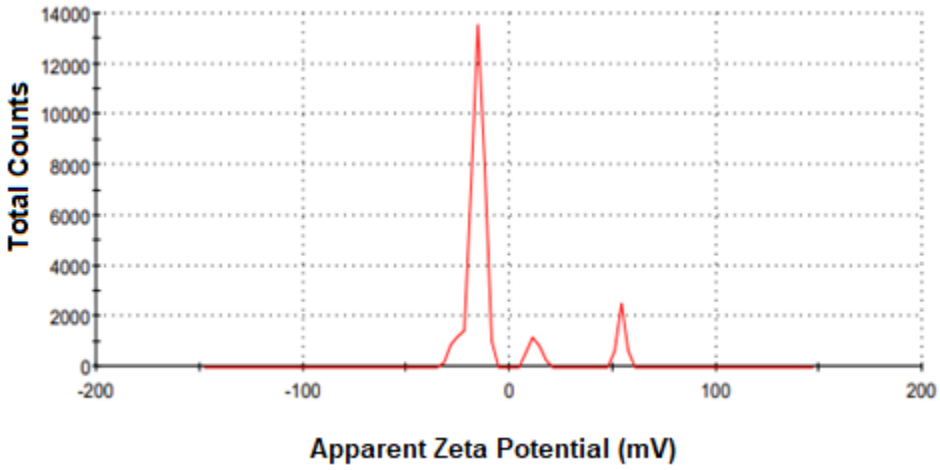

Fig. 8. Zeta potential assay of biosynthesized ZnO-NPs

Antimicrobial Activity

The antimicrobial properties of created ZnO-NPs by *H. pannosa* extracts have been assessed against different microorganisms. The tested microorganisms were chosen because they represented various microorganisms, including human pathogen bacteria, food spoilage bacteria, as well as human pathogen yeasts. The inhibition zones were recorded using 1000 µg/mL of synthesized ZnO-NPs and a broad spectrum antibiotic (azithromycin) (Table 2 and Fig. 9). As opposed to this, biosynthesized ZnO-NPs showed a strong antibacterial effect, which was on a par with azithromycin. The antibacterial activity of azithromycin had inhibition zones ranged from 0 to 25 mm, whereas ZnO-NPs had zones of inhibition from 22 to 27 mm. ZnO-NPs generated through *H. pannosa* showed

strong antibacterial efficacy *vs.* both infections in the present investigation. Antimicrobial activity ZnO-NPs was reported in other studies (Anjali *et al*. 2021; Alsalamah *et al*. 2023; Abdelhady *et al*. 2024).

Table 2. Antibacterial Activity of Biosynthesized ZnO-NPs

Strain Name	Diameter of Inhibition Zone (mm)		
	ZnO-NPs	Positive control	Negative control
Staphylococcus aureus	26	20	0
Enterococcus faecalis	27	25	0
Klebsiella pneumoniae	27	24	0
Acinetobacter baumannii	26	22	0
Candida albicans	23	0	0
Candida auris	22	0	0

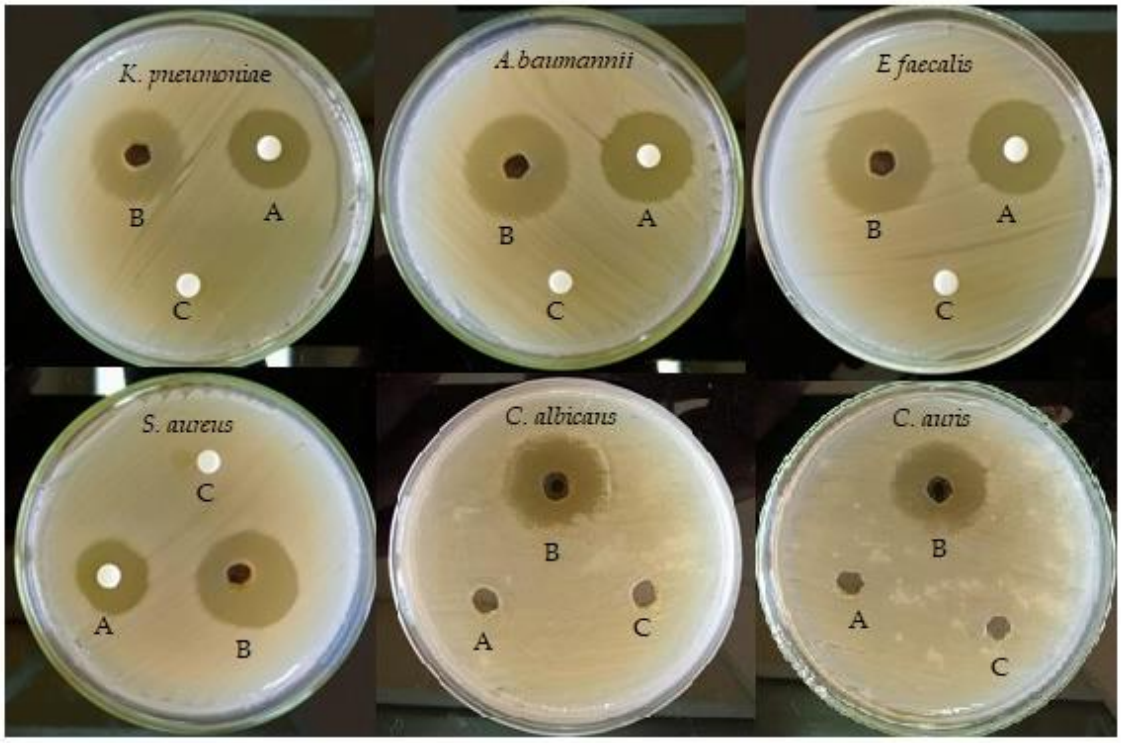

Fig. 9. Antimicrobial assay of biosynthesized ZnO-NPs, (A) positive control (B) ZnO-NPs and (C) negative control. Inhibition zones (mm)

For determination of MICs and MBCs of ZnO-NPs against *Staphylococcus aureus*, *Enterococcus faecalis, Klebsiella pneumoniae, Acinetobacter baumanii, Candida albicans*, and *Candida auris*, the inhibitory effect of different concentrations of Zn-ONPs (16.62-1000 µg/mL) were investigated (data not tabulated). Results showed that the MIC of ZnO-NPs was 12.5 µg/mL against almost all of the pathogenic microbes except for *Acinetobacter baumannii* in which the value was 25 µg/mL. The MBC value was 25 µg/mL against all tested microbes. Significant antibacterial activity was demonstrated for ZnO-NPs against *E. coli* as well as *E. faecalis*. Naturally occurring ZnO-NPs manufactured utilizing diverse biological components displayed varying antibacterial properties (Sukri *et al*. 2019; Abdelghany *et al*. 2023). Comparing ZnO-NPs created using cyanobacteria to conventionally manufactured ZnO-NPs, the former showed dose-dependent suppression

against *K. pneumoniae, S. aureus*, *B. cereus*, and *E. coli*, having MIC levels that ranged from 62.5 to 125 µg mL (Asif *et al*. 2021).

Anti-Biofilm Activity of ZnO-NPs

ZnO-NPs' anti-biofilm activity in the present research showed a range of results against different microorganisms. *Pseudomonas aeruginosa* was slightly inhibited by ZnO-NPs, with inhibition reaching 41.9% at 62.5 µg/mL, 31.31% at 31.25 µg/mL, 24.4% at 15.62 µg/mL, and 18.4% at 7.8 µg/mL. When used at concentrations below the minimum inhibitory concentration (MIC) value, ZnO-NPs, demonstrated the strongest inhibition of *Staphylococcus aureus* biofilm development without compromising growth of bacteria. The biofilm formation was decreased by 66.7%, 61.3%, 53.4%, and 46.9% at concentrations of 62.5, 31.25, 15.62, and 7.81 µg/mL, respectively (Fig. 10). According to a different study, naturally produced metal oxides prevent biofilm formation throughout the irreversible adhesion stage. At the MIC levels, there was inhibition of the initial biofilm formation (Ja yabalan *et al*. 2019). Another study assessed how metal oxide nanoparticles (NPs) can inhibit the biofilm formation of *E. coli* by interference with bacterial cell membranes along with inducing stress caused by oxidation (Kaweeteerawat *et al*. 2015).

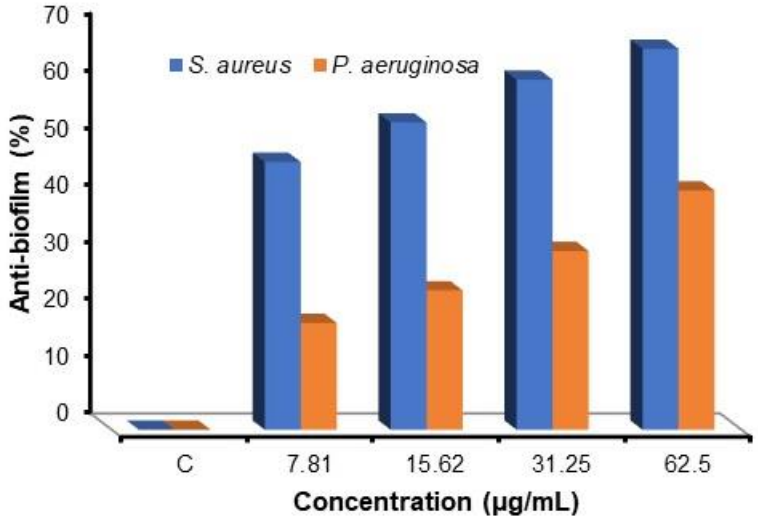

Fig. 10. Anti-biofilm assay of ZnO-NPs at different concentrations against Staphylococcus aureus and Pseudomonas aeruginosa. C, control (without ZnO-NPs)

Antiviral Activity of ZnO-NPs

ZnO-NPs' antiviral efficacy was assessed at their maximum non-toxic concentration (MNTC), which was found to be 31.2 µg/mL when tested against a vero standard cell line. The antiviral efficacy of ZnO-NPs was greater against HSV1 and COX B4 than COX B4 (Fig. 11). ZnO-NPs' antiviral efficacy against HSV1 was 61.1%, but it was 54.8% against COXB4. In this instance, ZnO-NPs have encouraging antiviral efficacy against COX B4 as well as HSV1, making them suitable for usage in biological applications. The antiviral efficacy of ZnO-NPs results from protein molecules as well as toll-type receptor pathways of signaling, and these in consequently stimulate the immune system's innate as well as adaptive mechanisms and cause the production of pro-inflammatory cytokines, which hinder the virus's replication (Melk *et al*. 2021).

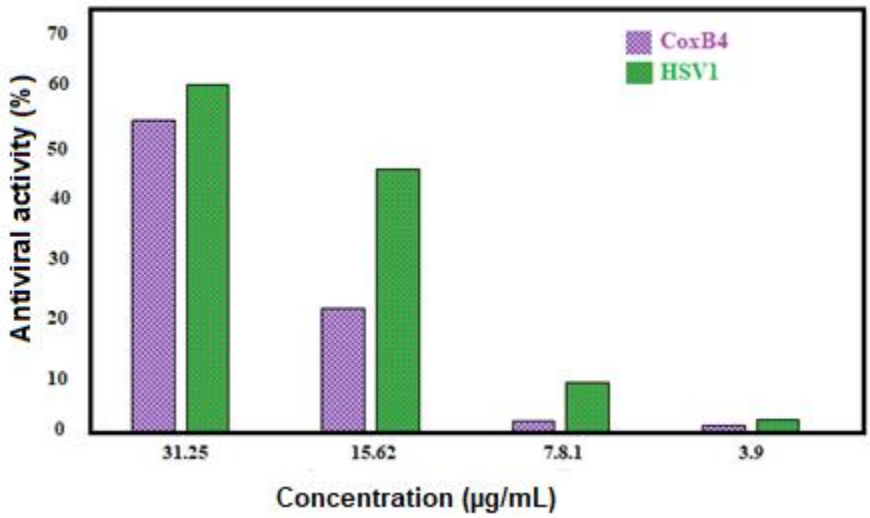

Fig. 11. Antiviral activity of ZnO-NPs against CoxB4 and HSV1 viruses

Antioxidant Activity of ZnO-NPs

ZnO-NPs demonstrated a modest level of DPPH radical-scavenging activity, whereas at 1000 µg/mL, it exhibited 85.6% inhibition, while at 1.95 µg/mL, it was 39.5%. Ascorbic acid was found to be 99.3% inhibiting at 1000 µg/mL, but the value was 43.7% at 1.95 µg/mL. Ascorbic acid often had more radical scavenging activity than ZnO-NPs. These findings suggest that ZnO-NPs depend on the dosage of radical scavenging substances (Chandra *et al*. 2019). The findings of phycosynthesized ZnO-NPs demonstrated their strong ability to scavenge radicals such as DPPH, with a successful antioxidant dosage required to achieve an IC_{50} value of 36.2 µg/mL (Fig. 12). The polyphenolic molecules which persisted on the outer layer of ZnO-NPs may be responsible for their antioxidant action; these bioactive compounds help donate hydrogen atoms to cause DPPH to change into its less concentrated form (Abdelghany *et al*. 2023).

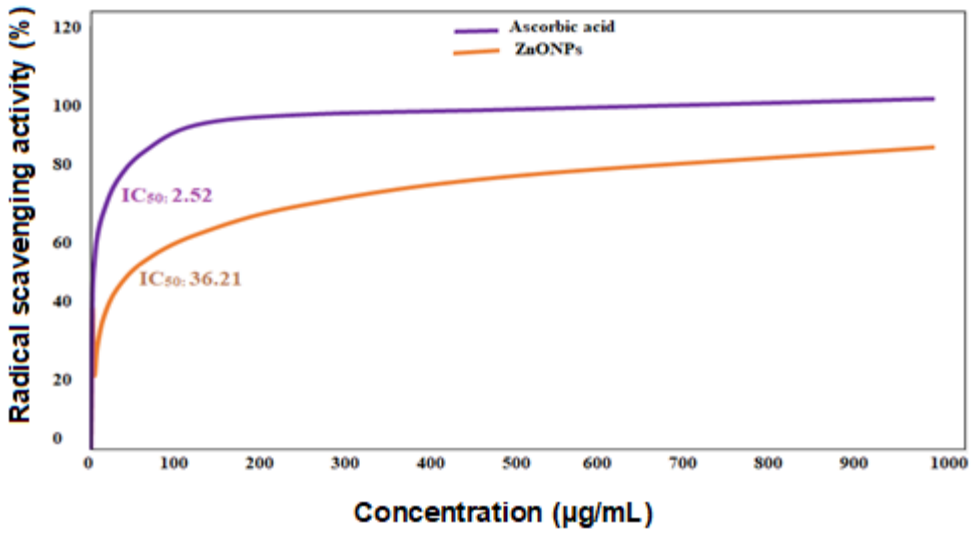

Fig. 12. Antioxidant activity of ascorbic acid and ZnO-NPs

Anti-inflammatory Activity of ZnO-NPs

The anti-inflammatory impact of ZnO-NPs and indomethacin (standard drug) was measured by inhibiting the destruction of RBC membranes generated by hypotonicity. According to data (Fig. 13), ZnO-NPs displayed a dosage-dependent anti-inflammatory activity, with the degree of protection depending on the used concentration. The ZnO-NPs substantially generated 93.3% suppression of RBC hemolysis at a dosage of 1000 µg/mL, compared to standard drug indomethacin. ZnO-NPs may maintain the membrane of red blood cells by stopping the expulsion of enzymes that are act lytic agent. Moreover, recent investigation demonstrated that ZnO-NPs possess anti-inflammatory and antioxidant activities (Nagajyothi *et al*. 2015; Al-Rajhi *et al*. 2022a, b).

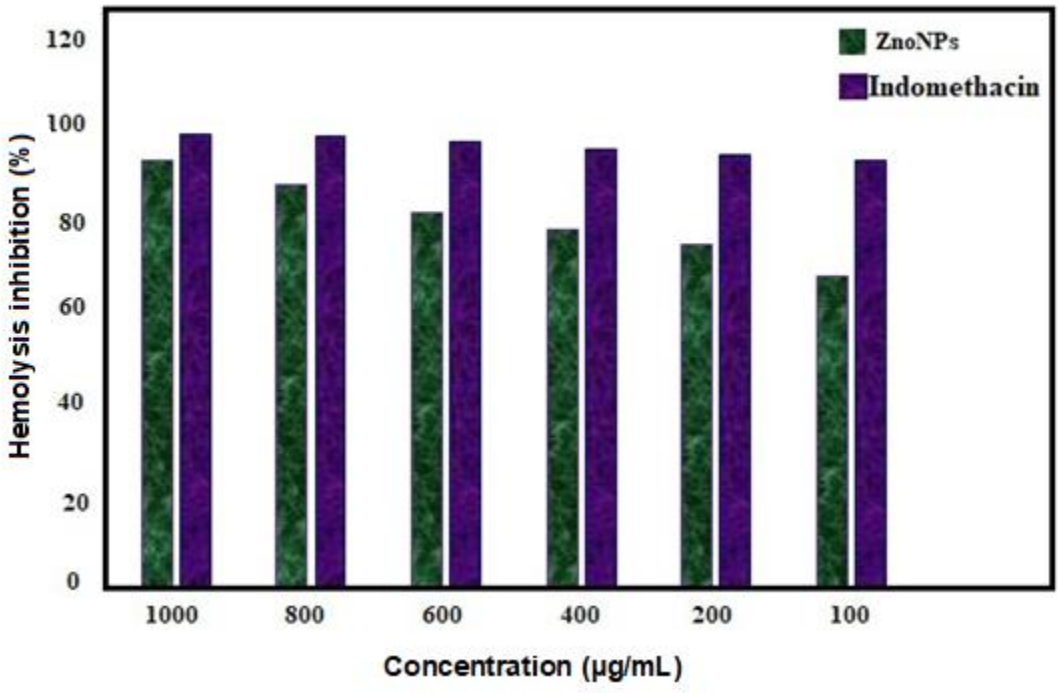

Fig. 13. Effect of ZnO-NPs and Stander Indomethacin on human red blood cell

Cytotoxicity and Antitumor Action of ZnO-NPs

The MTT experiment is a reliable colorimetric test used in cytotoxic and cell growth experiments to determine the total amount of viable cells. Exposure to various amounts of ZnO-NPs also caused dose-dependent cell death in both cancerous as well as healthy cells, as shown in (Fig. 14 A and B). More specifically, 109 µg/mL corresponds to the IC_{50} to feed renal Vero cells, which indicates normal cells. In contrast, the IC_{50} values for Pc3 and Caco2 in cancer cells were 83.3 µg/mL and 174.3 µg/mL, respectively. Therefore, it is strongly advised that ZnONP therapy be carried out at concentrations less than 109 µg/mL to maintain safety for humans. Cytotoxicity of ZnO-NPs synthesized by *Punica granatum* was investigated (Sukri *et al*. 2019) against human colon normal and cancerous cells, where similar killing potential was observed on both cell lines at dose of ≥31.2 µg/mL.

Many investigations have indicated that ZnO-NPs have anticancer activity towards various cancer cell types; however, the degree of toxicity was different depending on the size and the production source of nanoparticles. For instance, the anticancer effect of eco-

friendly synthesized ZnO-NPs against PC3 cells was recorded (Rahimi *et al*. 2020). Also, ZnO-NPs reflected strong anticancer activity towards carcinoma of the breast cell lines. Induction of Huh-7 carcinoma cells apoptosis was observed as a result of cells exposure to ZnO-NPs (Mohammadi *et al*. 2022).

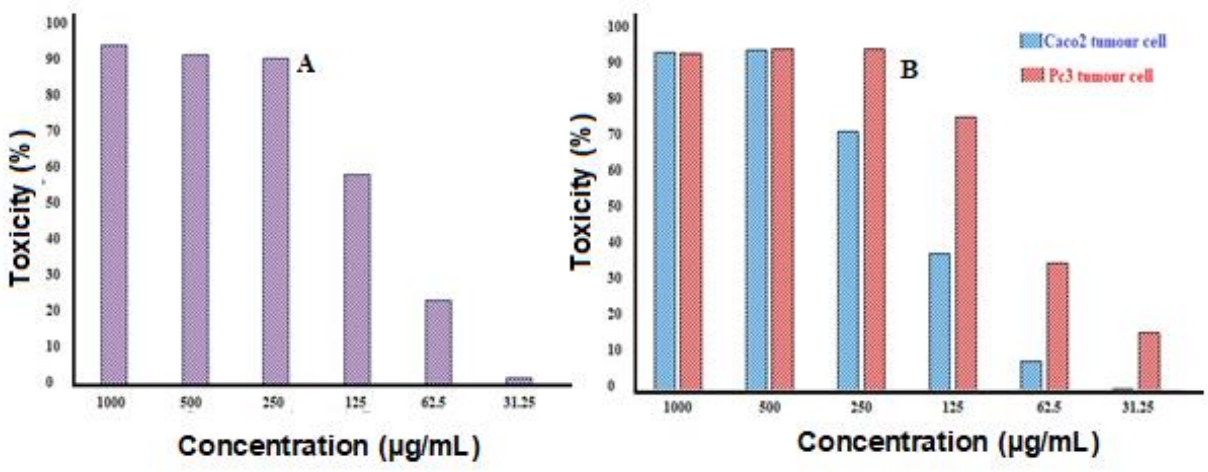

Fig. 14. Cytotoxicity of ZnO-NPs against normal vero cells (A) and cancer cells (B)

CONCLUSIONS

1. The highest percentage of the algal extract was associated with hexadecanoic acid (25.7%) and isopropyl myristate (18.3%).
2. *Via* 2,2-diphenyl-1-picrylhydrazyl (DPPH) radical-scavenging activity, the created ZnO-NPs demonstrated strong antioxidant activity with IC_{50} value of 36.2 µg/mL.
3. ZnO-NPs exhibited excellent antimicrobial activity against *Staphylococcus aureus*, *Enterococcus faecalis*, *Klebsiella pneumoniae*, *Acinetobacter baumannii*, *Candida albicans*, and *Candida auris* with excellent inhibition zones besides anti-inflammatory activity. Moreover, a promising antiviral activity against HSV1 and COX B4 viruses, anti-biofilm against *S. aureus* and *P. aeruginosa*, and antitumour against Pc3 and Caco2 cancer cells were recorded.
4. ZnO-NPs produced by *H. pannosa* may be used as an alternative for traditional antibiotics; however, more investigations are required to determine its toxicity.

ACKNOWLEDGMENTS

The authors extend their appreciation to the Deputyship for Research & Innovation, Ministry of Education in Saudi Arabia for funding this research work through the project number ISP-2024.

REFERENCES CITED

Abdel Ghany, T. M., Al-Rajhi A. M., Mohamed, A. A., Alawlaqi, M. M., Magdah, M., Helmy E., M., and Ahmed S. M. (2018). "Recent advances in green synthesis of silver nanoparticles and their applications: About future directions. A Review," *BioNanoSci*. 8(1), 5-16. DOI 10.1007/s12668-017-0413-3

Abdel Ghany, T. M., Ganash, M., Bakri, M. M., Qanash, H., Al-Rajhi, A. M., and Elhussieny, N. I. (2021). "A review SARS-CoV-2 the other face to SARS-CoV and MERS-CoV: About future predictions," *Biomedical Journal* 44(1), 86-93. DOI: 10.1016/j.bj.2020.10.008

Abdelghany, T. M., Al-Rajhi, A. M. H., Yahya, R. *et al.* (2023a). "Phytofabrication of zinc oxide nanoparticles with advanced characterization and its antioxidant, anticancer, and antimicrobial activity against pathogenic microorganisms," *Biomass Conv. Bioref.* 13, 417-430. DOI: 10.1007/s13399-022-03412-1

Abdelhady, M. A., Abdelghany, T. M., Mohamed, S. H., and Abdelbary, S. A. (2024). "Impact of green synthesized zinc oxide nanoparticles for treating dry rot in potato tubers," *BioResources* 19(2), 2106-2119. DOI: 10.15376/biores.19.2.2106-2119

Agarwal, H., Kumar, S. V., and Rajeshkumar, S. (2017). "A review on green synthesis of zinc oxide nanoparticles–An eco-friendly approach," *Resource-Efficient Technologies* 3(4), 406-413. DOI: 10.1016/j.reffit.2017.03.002

Alawlaqi, M. M., Al-Rajhi A. M. H., Abdelghany, T. M., Ganash, M., and Moawad, H. (2023). "Evaluation of biomedical applications for linseed extract: Antimicrobial, antioxidant, anti-diabetic, and anti-inflammatory activities *in vitro*," *Journal of Functional Biomaterials* 14(6), 300. DOI: 10.3390/jfb14060300

Alghonaim, M. I., Alsalamah, S. A., Alsolami, A., and Abdelghany, T. M. (2023). "Characterization and efficiency of *Ganoderma lucidum* biomass as an antimicrobial and anticancer agent," *BioResources* 18(4), 8037-8061. DOI: 10.15376/biores.18.4.8037-8061

Alghonaim, M. I., Alsalamah, S. A., Ali, Y., and Abdelghany, T. M. (2024a). "Green mediator for selenium nanoparticles synthesis with antimicrobial activity and plant biostimulant properties under heavy metal stress," *BioResources* 19(1), 898-916. DOI: 10.15376/biores.19.1.898-916

Alghonaim, M. I., Alsalamah, S. A., Mohammad, A. M., and Tarek, M. Abdelghany. (2024b). "Green synthesis of bimetallic Se@TiO_2NPs and their formulation into biopolymers and their utilization as antimicrobial, anti-diabetic, antioxidant, and healing agent in vitro," *Biomass Conv. Bioref.* Early access. DOI: 10.1007/s13399-024-05451-2

Al-Rajhi, A. M. H., Yahya, R., Alawlaqi, M. M., Fareid, M. A., Amin, B. H., and Abdelghany, T. M. (2022a). "Copper oxide nanoparticles as fungistat to inhibit mycotoxins and hydrolytic enzyme production by *Fusarium incarnatum* isolated from garlic biomass," *BioResources* 17(2), 3042-3056. DOI: 10.15376/biores.17.2.3042-3056

Al-Rajhi, A. M. H., Yahya, R., and Bakri, M. M. (2022b). "*In situ* green synthesis of Cu-doped ZnO based polymers nanocomposite with studying antimicrobial, antioxidant and anti-inflammatory activities," *Appl. Biol. Chem.* 65, article no. 35. DOI: 10.1186/s13765-022-00702-0

Al-Rajhi, A. M. H., and Abdelghany, T. M. (2023). "*In vitro* repress of breast cancer by bio-product of edible *Pleurotus ostreatus* loaded with chitosan nanoparticles," *Appl. Biol. Chem.* 66, article 33. DOI: 10.1186/s13765-023-00788-0

Alsalamah, S. A., Alghonaim, M. I., Mohammad, A. M., and Abdel Ghany, T. M. (2023). "Algal biomass extract as mediator for copper oxide nanoparticle synthesis: Applications in control of fungal, bacterial growth, and photocatalytic degradations of dyes," *BioResources* 18(4), 7474-7489. DOI: 10.15376/biores.18.4.7474-7489

Alsolami, A., Bazaid, A. S., Alshammari, M. A., Qanash, H., Amin, B. H., Bakri, M. M., and Abdelghany, T. M. (2023). "Ecofriendly fabrication of natural jojoba nanoemulsion and chitosan/jojoba nanoemulsion with studying the antimicrobial, anti-biofilm, and anti-diabetic activities *in vitro*," *Biomass Conv. Bioref.* DOI: 10.1007/s13399-023-05162-0

Anjali, K. P., Sangeetha, B. M., Raghunathan, R., Devi, G., and Dutta, S. (2021). "Seaweed mediated fabrication of zinc oxide nanoparticles and their antibacterial, antifungal and anticancer applications," *ChemistrySelect* 6(4), 647-656. DOI: 10.1002/slct.202003517

Anosike, C. A., Obidoa, O. and Ezeanyika, L. U. (2012). "Membrane stabilization as a mechanism of the anti-inflammatory activity of methanol extract of garden egg (*Solanum aethiopicum*)," *DARU Journal of Pharmaceutical Sciences* 20(1), article 76. DOI: 10.1186/2008-2231-20-76

Ansari, S., Nepal, H. P., Gautam, R., Shrestha, S., Neopane, P., Gurung, G., and Chapagain, M. L. (2015). "Community acquired multi-drug resistant clinical isolates of *Escherichia coli* in a tertiary care center of Nepal," *Antimicrobial Resistance and Infection Control* 4, 15, DOI: 10.1186/s13756-015-0059-2

Ashajyothi, C., Harish, K. H., Dubey, N., and Chandrakanth, R. K. (2016). "Antibiofilm activity of biogenic copper and zinc oxide nanoparticles-antimicrobials collegiate against multiple drug resistant bacteria: A nanoscale approach," *Journal of Nanostructure in Chemistry* 6, 329-341. DOI: 10.1007/s40097-016-0205-2

Asif, N., Fatima, S., Aziz, M. N., Zaki, A., and Fatma, T. (2021). "Biofabrication and characterization of cyanobacteria derived ZnO NPs for their bioactivity comparison with commercial chemically synthesized nanoparticles," *Bioorganic Chemistry* 113, article 104999. DOI: 10.1016/j.bioorg.2021.104999

Azizi, S., Ahmad, M. B., Namvar, F., and Mohamad, R. (2014). "Green biosynthesis and characterization of zinc oxide nanoparticles using brown marine macroalga *Sargassum muticum* aqueous extract," *Materials Letters* 116, 275-277. DOI: 10.1016/j.matlet.2013.11.038

Chandra, H., Patel, D., Kumari, P., Jangwan, J. S., and Yadav, S. (2019). "Phyto-mediated synthesis of zinc oxide nanoparticles of *Berberis aristata*: Characterization, antioxidant activity and antibacterial activity with special reference to urinary tract pathogens," *Materials Science and Engineering: C* 102, 212-220. DOI: 10.1016/j.msec.2019.04.035

Elrefaey, A. A. K., El-Gamal, A. D., Hamed, S. M., and El-Belely, E. F. (2022). "Algae-mediated biosynthesis of zinc oxide nanoparticles from *Cystoseira crinite* (Fucales; Sargassaceae) and it's antimicrobial and antioxidant activities," *Egyptian Journal of Chemistry* 65(4), 231-240. DOI: 10.21608/EJCHEM.2021.87722.4231

Hemaid, A. S. S., Abdelghany, M. M. E. and Abdelghany, T. M. (2021). "Isolation and identification of Candida spp. from immunocompromised patients," *Bull Natl Res Cent* 45, 163. DOI: 10.1186/s42269-021-00620-z.

Jan, H., Shah, M., Usman, H., Khan, M. A., Zia, M., Hano, C., and Abbasi, B. H. (2020). "Biogenic synthesis and characterization of antimicrobial and antiparasitic zinc oxide (ZnO) nanoparticles using aqueous extracts of the Himalayan Columbine (*Aquilegia pubiflora*)," *Frontiers in Materials* 7, p. 249. DOI: 10.3389/fmats.2020.00249

Jayabalan, J., Mani, G., Krishnan, N., Pernabas, J., Devadoss, J. M., and Jang, H. T. (2019). "Green biogenic synthesis of zinc oxide nanoparticles using *Pseudomonas putida* culture and its *in vitro* antibacterial and anti-biofilm activity," *Biocatalysis and Agricultural Biotechnology* 21, article 101327. DOI: 10.1016/j.bcab.2019.101327

Kalaba, M. H., Moghannem, S. A., El-Hawary, A. S., Radwan, A. A., Sharaf, M. H., and Shaban, A. S. (2021). "Green synthesized ZnO nanoparticles mediated by *Streptomyces plicatus*: Characterizations, antimicrobial and nematicidal activities and cytogenetic effects," *Plants* 10(9), 1760. DOI: 10.3390/plants1009176

Kaur, J., Anwer, M. K., Sartaj, A., Panda, B. P., Ali, A., Zafar, A., Kumar, V., Gilani, S. J., Kala, C., and Taleuzzaman, M. (2022). "ZnO nanoparticles of *Rubia cordifolia* extract formulation developed and optimized with QbD application, considering ex vivo skin permeation, antimicrobial and antioxidant properties," *Molecules* 27(4), article 1450. DOI: 10.3390/molecules27041450

Kaweeteerawat, C., Ivask, A., Liu, R., Zhang, H., Chang, C. H., Low-Kam, C., and Godwin, H. (2015). "Toxicity of metal oxide nanoparticles in *Escherichia coli* correlates with conduction band and hydration energies," *Environmental Science and Technology* 49(2), 1105-1112. DOI: 10.1021/es504259s

Khan, S. T., Musarrat, J., and Al-Khedhairy, A. A. (2016). "Countering drug resistance, infectious diseases, and sepsis using metal and metal oxides nanoparticles: Current status," *Colloids and Surfaces B: Biointerfaces* 146, 70-83. DOI: 10.1016/j.colsurfb.2016.05.046

Marsalek, R. (2014). "Particle size and zeta potential of ZnO," *APCBEE Procedia* 9, 13-17. DOI: 10.1016/j.apcbee.2014.01.003

Melk, M. M., El-Hawary, S. S., Melek, F. R., Saleh, D. O., Ali, O. M., El Raey, M. A., and Selim, N. M (2021). "Antiviral activity of zinc oxide nanoparticles mediated by *Plumbago indica* L. extract against Herpes Simplex Virus Type 1 (HSV-1)," *International Journal of Nanomedicine* 16, 8221-8233. DOI: 10.2147/IJN.S339404

Mohammadi, S. A. F., Tafvizi, F. and Noorbazargan, H. (2022). "Anti-cancer effects of biosynthesized zinc oxide nanoparticles using *Artemisia scoparia* in Huh-7 liver cancer cells," *Inorganic and Nano-Metal Chemistry* 52(3), 375-386, DOI: 10.1080/24701556.2021.1980018

Nagajyothi, P. C., Cha, S. J., Yang, I. J., Sreekanth, T. V. M., Kim, K. J., and Shin, H. M. (2015). "Antioxidant and anti-inflammatory activities of zinc oxide nanoparticles synthesized using *Polygala tenuifolia* root extract," *Journal of Photochemistry and Photobiology B: Biology* 146, 10-17. DOI: 10.1016/j.jphotobiol.2015.02.008

Nagaraja, A., Jalageri, M. D., Puttaiahgowda, Y. M., Reddy, K. R., and Raghu, A. V. (2019). "A review on various maleic anhydride antimicrobial polymers," *Journal of Microbiological Methods* 163, article 105650. DOI: 10.1016/j.mimet.2019.105650

Nagarajan, S., and Arumugam, K. (2013). "Extracellular synthesis of zinc oxide nanoparticle using seaweeds of gulf of Mannar, India," *Journal of Nanobiotechnology* 11(39), 1-11. DOI: 10.1186/1477-3155-11-39

Naseer, M., Aslam, U., Khalid, B., and Chen, B. (2020). "Green route to synthesize zinc oxide nanoparticles using leaf extracts of *Cassia fistula* and *Melia azadarach* and

their antibacterial potential," *Scientific Reports* 10(1), article 9055. DOI: 10.1038/s41598-020-65949-3

Priyadharshini, R. I., Prasannaraj, G., Geetha, N., and Venkatachalam, P. (2014). "Microwave-mediated extracellular synthesis of metallic silver and zinc oxide nanoparticles using macro-algae (*Gracilaria edulis*) extracts and its anticancer activity against human PC3 cell lines," *Applied Biochemistry and Biotechnology* 174, 2777-2790. DOI: 10.1007/s12010-014-1225-3

Qanash, H., Bazaid, A. S., Alharazi, T., Barnawi, H., Alotaibi, K., Shater, A. R. M., and Abdelghany, T. M. (2023). "Bioenvironmental applications of myco-created bioactive zinc oxide nanoparticle-doped selenium oxide nanoparticles," *Biomass Conversion and Biorefinery* 2023, 1-12. DOI: 10.1007/s13399-023-03809-6

Qanash, H., Yahya, R., Bakri, M. M., Bazaid, A. S., Qanash, S., Shater, A. F., and Abdelghany, T. M. (2022). "Anticancer, antioxidant, antiviral and antimicrobial activities of Kei Apple (*Dovyalis caffra*) fruit," *Sci. Rep.* 12(1), article 5914. DOI: 10.1038/s41598-022-09993-1

Rahimi, K. S., Mohammad, G., Karimi, E., Oskoueian, E., and Homayouni-Tabrizi, M. (2020). "Anticancer properties of green-synthesised zinc oxide nanoparticles using *Hyssopus officinalis* extract on prostate carcinoma cells and its effects on testicular damage and spermatogenesis in Balb/C mice," *Andrologia* 52(1), article e13450. DOI: 10.1111/and.13450

Rahimi Kalateh Shah Mohammad, G., Karimi, E., Oskoueian, E., and Homayouni-Tabrizi, M. (2020). "Anticancer properties of green-synthesised zinc oxide nanoparticles using *Hyssopus officinalis* extract on prostate carcinoma cells and its effects on testicular damage and spermatogenesis in Balb/C mice," *Andrologia* 52(1), article e13450. DOI: 10.1111/and.13450

Romdhane, A., Aurousseau, M., Guillet, A., & Mauret, E. (2015). "Effect of pH and ionic strength on the electrical charge and particle size distribution of starch nanocrystal suspensions," *Starch-Stärke* 67(3-4), 319-327. DOI: 10.1002/star.201400181

Salama, A. M., Helmy, E. A., and Abd El-ghany, T. M. (2021). "Nickel oxide nanoparticles application for enhancing biogas production using certain wastewater bacteria and aquatic macrophytes biomass," *Waste Biomass Valor* 12, 2059-2070 DOI: 10.1007/s12649-020-01144-9

Siddiqi, K. S., ur Rahman, A., Tajuddin, N., and Husen, A. (2018). "Properties of zinc oxide nanoparticles and their activity against microbes," *Nanoscale Research Letters* 13(141), 1-13. DOI: 10.1186/s11671-018-2532-3

Singh, N. A., Narang, J., Garg, D., Jain, V., Payasi, D., Suleman, S., and Swami, R. K. (2023). "Nanoparticles synthesis via microorganisms and their prospective applications in agriculture," *Plant Nano Biology* 5, article 100047. DOI: 10.1016/j.plana.2023.100047

Sukri, S. N., Shameli, K., Wong, M. M. T., Teow, S. Y., Chew, J., and Ismail, N. A. (2019). "Cytotoxicity and antibacterial activities of plant-mediated synthesized zinc oxide (ZnO) nanoparticles using *Punica granatum* (pomegranate) fruit peels extract," *Journal of Molecular Structure* 1189, 57-65. DOI: DOI: DOI: 10.1016/j.molstruc.2019.04.026

Talam, S., Karumuri, S. R., and Gunnam, N. (2012). "Synthesis, characterization, and spectroscopic properties of ZnO nanoparticles," *International Scholarly Research Notices* article 2012 article 372505. DOI: 10.5402/2012/372505

Waters, E. M., Rowe, S. E., O'Gara, J. P., and Conlon, B. P. (2016). "Convergence of *Staphylococcus aureus* persister and biofilm research: can biofilms be defined as communities of adherent persister cells?," *PLoS Pathogens* 12(12), article e1006012. DOI: 10.1371/journal.ppat.1006012

Yahya R, Al-Rajhi, A. M. H., Alzaid, S. Z., Al Abboud, M. A., Almuhayawi, M. S., Al Jaouni, S. K., Selim, S., Ismail, K. S., and Abdelghany, T. M. (2022). "Molecular docking and efficacy of *Aloe vera* gel based on chitosan nanoparticles against *Helicobacter pylori* and its antioxidant and anti-inflammatory activities," *Polymers* 14(15), 2994. DOI: 10.3390/polym14152994

Yakubu, E., Otitoju, O., and Onwuka, J. (2017). "Gas chromatography-mass spectrometry (GC-MS) analysis of aqueous extract of *Daniellia oliveri* stem bark," *Pharmaceutica Analytica Acta* 8(11), article 568. DOI: 10.4172/2153-2435.1000568

Article submitted: March 18, 2024; Peer review completed: April 6, 2024; Revised version received: April 10, 2024; Accepted: April 11, 2024; Published: April 26, 2024.
DOI: 10.15376/biores.19.2.3771-3792